Paper No.
00000 **(Official use)**

N-benzylidine-2(2-oxo-2-(10H-phenothiazine-10yl) amino) acetohydrazide as environmentally benign corrosion inhibitor for mild steel in 1M HCl solution

Mohammad Mobin
Corrosion Research Laboratory, Applied Chemistry Department
Aligarh Muslim University, Aligarh, U.P, India
Email: *drmmobin@hotmail.com*

Saman Zehra
Corrosion Research Laboratory, Applied Chemistry Department
Aligarh Muslim University, Aligarh, U.P, India

ABSTRACT

In the present study, we are reporting the investigation of an environmentally benign compound, a glycine derivative N-benzylidine-2((2-oxo-2-(10H-phenothiazine-10yl) amino) acetohydrazide (BPAA), as potential corrosion inhibitor for mild steel in 1M HCl solution at temperatures 30-60°C. The investigation is accomplished by electrochemical polarization, electrochemical impedance spectroscopy (EIS), gravimetric, UV-visible spectrophotometry, FT-IR spectroscopy and scanning electron microscopy (SEM). The evaluated compound works as effective inhibitor for acid corrosion at substantially lower concentration and its adsorption on the MS surface was found to obey the Langmuir adsorption isotherm. Calculated thermodynamic parameters for adsorption unveiled a strong interaction amongst the inhibitor-mild steel surface. The electrochemical results revealed that the inhibitor act as mixed-type. The order of IE acquired from experimental results is successfully verified by theoretical calculations.

Keywords: Corrosion Inhibitor; EIS; SEM; EDS; DFT; Synergistic effect

INTRODUCTION

Mild Steel (MS) has been substantially used as a material of choice in wide variety of industrial applications because of its adequate mechanical properties, ease of accessibility and economic consideration, such as in petroleum refineries, storage tank, reaction vessels etc[1]. However, disadvantage of the poor 'corrosion resistance' in aggressive solutions confines the application of MS without adequate protection. Strong mineral acids like HCl are generally used in several industrial processes, such as removal of rust in metal finishing industries, steel pickling, acid descaling etc., which usually results in serious MS corrosion, if used unprotected[2]. In order to mitigate the adverse consequences of the solution and to retard MS corrosion, addition of several additives or inhibitors in small concentration is a very guaranteeing and insightful approach[3]. Both organic and inorganic compounds have been substantially used as excellent inhibitors but the use of inorganic compounds is usually undesirable due to their toxicity and environmental hazardness. In this connection, organic compounds incorporating electron rich functional groups along with π-electrons display much better corrosion inhibition efficiency. These inhibitors work by anodic mechanism i.e. by forming protective film, which avoids the diffusion of corrosion causing ions from solution to the metal. Organic molecules having N, O and S donor sites, (-electrons and conjugated aromatic rings adsorb more effectively because of their capability to donate available lone pair of electrons or accept back donated electron density in the antibonding orbitals[4]. Although being versatile in terms of effectiveness and eco-friendliness, most of the commonly exploited organic corrosion inhibitors are expensive and thus needs to be replaced by inexpensive and environment-friendly compounds. This has led to the research of a range of environmentally benign organic compounds as effective corrosion inhibitors[5]. In recent years, the exploration for new eco-friendly compounds as potential inhibitors has encouraged the evaluation of different amino acids and their derivatives as safe inhibitors for corrosion of different metals in various aggressive media[6,7]. However, the employment of single amino acids have the limitation of high amount of usage and low to moderate IE[8]. Attempts have already been made to further enhance the corrosion inhibition performance of amino acids by incorporating substances having synergistic effect such as halide additives[9]. Mobin et al[6,7,10] in a sequence of papers have reported that inhibiting effect of some amino acids can further be improved by synergizing them with surfactants additives. In extension to our previous research we are reporting the studies pertaining to the inhibition influence of phenothiazine derivative of the glycine (BPAA) for corrosion of MS in acid medium. Phenothiazine with two donor atoms in its core have been claimed as green corrosion inhibitor with moderate IE[11]. The relevant literature also suggests that phenothiazine and its several derivatives can be quickly and easily synthesized from relatively cheap commercially available chemicals[12,13]. However, amino acid glycine has been observed to moderately inhibit (72% IE at 0.1M glycine) corrosion of MS in HCl solution at high concentration[14]. At lower concentration, however, it accelerated the corrosion for MS. For Cu corrosion in HNO_3 glycine accelerated corrosion at all the examined concentrations [15]. Because of these findings, it was thought worthwhile to synthesize BPAA, to investigate it as inhibitor on corrosion of MS in acidic medium. The presence of nitrogen, sulfur and oxygen atoms and aromatic ring in its structure, BPAA is expected to get easily adsorbed on the MS surface and work as excellent corrosion inhibitor.

EXPERIMENTAL PROCEDURE

SYNTHESIS OF THE BPAA

BPAA) analyzed in the evaluation was synthesized based on a route earlier reported (Scheme 1)[12,13].

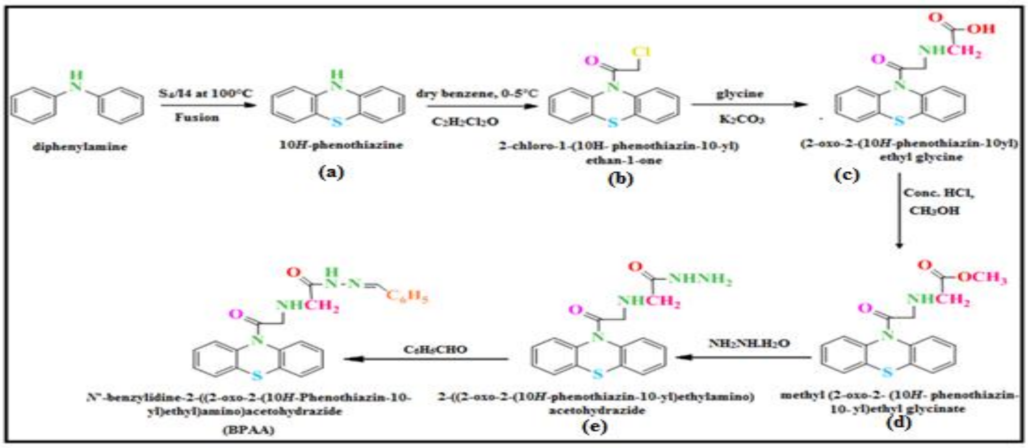

Scheme 1: Scheme for the preparation of BPAA.

Table 1: Chemical structure and spectral data of the BPAA.

Structure	**IR(KBr), cm^{-1}**	**ELEMENTAL ANALYSIS, %**
	1680 cm^{-1} (Phenothiazine ring), 1638 cm^{-1} (C=O), 2939 cm^{-1} (CH_2), 2925.46 cm^{-1} (NH), 1407.5 cm^{-1} (C-N), 1588.89 cm^{-1} (Ar-C=C), 3433.11 cm^{-1}(Ar-phenyl ring)	**Cal.**: C(67.54), H(5.44) N(12.60, O(7.95), S(7.97) **Found**: C(64.98), H (4.85), N(11.96), O(9.58), S(8.99)

REPARATION OF METAL SPECIMEN AND TEST SOLUTION

For gravimetric studies MS coupons of size (2.5 X 2.0 X 0.03 cm) and for electrochemical measurements circular specimens of diameter 1 cm^2 were used. The specimens were machined and abraded with a series of emery papers (grade 320-1200), followed by rinsing with acetone as well as with double distilled water and then dried in warm air.

The aggressive test solution (1M HCl) was prepared by the dilution of analytical grade 35% HCl with double distilled water. Inhibitors were dissolved in acid solution at required concentrations in ppm and the solution in the absence of inhibitor was taken as blank for comparison purposes.

ELECTROCHEMICAL MEASUREMENTS

The electrochemical measurements were carried out on AutolabPotentiostat/Galvanostat, model 128N with inbuilt impedance analyzer FRA2. The experiments were carried out using a corrosion cell from Autolab with Ag/AgCl electrode (saturated KCl) as reference electrode, Pt wire as counter electrode and MS specimens with exposed surface area of 1 cm^2 as working electrode. A Luggin-Haber capillary was also included in the cell set up and the tip of the capillary was kept very close to the surface of the working electrode to minimize IR drop. The specimens were allowed to stabilize in the test solution for 30 min prior to the experiments. All the experiments were done at room temperature (30±1°C). The potentiodynamic polarization (PDP) measurements were performed at a scan rate of 0.001 V/s in the potential range of 0.250V below the corrosion potential to 0.250V above the corrosion potential. Electrochemical Impedance Spectroscopy (EIS) was implemented at open circuit potential within frequency range of 10^{-2} to 10^{5} Hz with 10mV perturbation.

GRAVIMETRIC STUDY

After accurate weighing, the freshly prepared mild steel coupons were suspended in 250 ml beakers containing 200 ml of test solution maintained at 30-60°C using a thermo-stated water bath.After completion of 6 h of immersion, the coupons were taken out, the corrosion products were removed from the surface, dried and then the specimens were again weighed and the difference in weight was recorded. The weight loss taken was the difference between the weight at a given time and the original weight of the specimen. The corrosion rate was determined using the following equation[7]:

$$v = \frac{\Delta W}{At} \tag{1}$$

$$\eta_w\,(\%) = \frac{v_o - v_i}{v_o} \times 100 \tag{2}$$

where ΔW is the weight loss in mg, *A* is area of coupon, *t* is immersion time, and v_o and v_i are the corrosion rates in absence and presence of inhibitor. Surface coverage (θ) was evaluated at constant temperature and for different concentrations of inhibitor in 1 M HCl from weight loss measurements according to equation:

$$\theta = \frac{v_o - v_i}{v_o} \tag{3}$$

UV–VISIBLE SPECTROSCOPY

UV–visible study was carried out for 100 ppm of BPAA in 1M HCl before and after 6 h of MS immersion utilizing a Perkin–Elmer UV–visible spectrophotometer, Lambda 25, in order to confirm, the possibility of the formation of inhibitor-metal complex.

FT-IR SPECTROSCOPY

FT-IR spectra of pure BPAA and BPAA adsorbed on the MS surface in 1M HCl solution were acquired using FT-IR (Model: PerkinElmer Spectrum Version 10.4.00) in the frequency range of 4000-500 cm^{-1}. For which the MS specimen was first immersed in 1 M HCl solution with 100 ppm of inhibitor at 30 °C, 6 h post immersion, the sample was taken out, corrosion product scrapped from the surface, dried in vacuum for 48 h and subjected to FT-IR analysis.

SEM/EDX

For SEM/EDX, MS coupons obtained after gravimetric experiments with and without an optimum concentration of inhibitor, were used. The samples were analyzed using JEOL (Japan) SEM (Model: JSM- 6510LV) attached with an Oxford Instruments EDX Analysis System, INCA 300 (UK), in order to visualize the severity of corrosion damage to the MS specimens in uninhibited/inhibited acid solution in terms of surface heterogeneity/roughness.

QUANTUM CHEMICAL CALCULATIONS

Theoretical calculation were carried out by DFT calculations using the ORCA programme module (version 3.0.3) by using the Becke's three parameter hybrid, B3LYP and full optimization was performed with SVP/SV(J) basis set. The calculated parameters are, the energy of the highest occupied molecular orbital (E_{HOMO}), the lowest unoccupied molecular orbital (E_{LUMO}), the separation energy (ΔE) and the total energy (E_t).

RESULTS

ELECTROCHEMICAL MEASUREMENTS

The Tafel plots (current-potential relationship) for MS in 1M HCl without and with different concentration of BPAA are shown in Figure 1 A. Different electrochemical kinetic parameters deduced from polarization curves like corrosion potential (E_{corr}), corrosion current density (i_{corr}), the cathodic Tafel slope (β_c), and the anodic Tafel slope (β_a) are shown in Table 1. Addition of inhibitors is seen to affect the anodic and cathodic reaction, shifting the value of corrosion potential (E_{corr}) slightly toward anodic value (more positive) but no definite shift in E_{corr} detected and reducing the cathodic and anodic current densities and the corresponding corrosion current density (i_{corr})[13]. Which indicates that the investigated inhibitor act as mixed type in the acid solution. The value of i_{corr} decreases in presence of inhibitor.

To estimate %IE, the values of corrosion current densities in the absence and presence of inhibitor were used by using following equation[6]:

$$\%\text{IE} = \left(\frac{i^{\circ}_{corr} - i_{corr}}{i^{\circ}_{corr}} \right) \times 100 \tag{4}$$

where, i_{corr}° and i_{corr} are the corrosion current density in presence and absence of the inhibitor. The obtained values are also listed in Table 1 and follow the same trend as the gravimetric and EIS data.

Nyquist plots in 1M HCl at 30°C were obtained and presented in Figure 1 B. The Nyquist plots show single capacitive loop, which is attributed to the charge transfer of the corrosion process. The diameter of the loops increases with increasing BPAA concentration which is attributed to the charge transfer of the corrosion process. The capacitive loops are not exact semi circles but depressed to some extent, which is attributed to the frequency dispersion effect due to roughness and inhomogeniety of electrode surfaces, indicating the adsorption of inhibitor molecules and exhibiting a barrier effect that would effectively protect the metal from aggressive attack by the solution. Considering the above facts, the impedance plots are fitted with equivalent circuit with one time constant, as shown in Figure 1 C, which includes solution resistance, R_s and double layer capacitance, C_{dl}, which is placed in parallel to charge transfer resistance, R_{ct}. To get more accurate semicircle fit CPE is substituted for double layer capacitance, C_{dl} as metal/solution interface does not correspond to an ideal capacitor. The EIS parameters are given in Table 1. The main parameters obtained from EIS measurements are R_{ct} and C_{dl}. A decrease in C_{dl} values with accompanying increase in R_{ct} values, in general, suggest that corrosion inhibition performance of BPAA for MS in 1M HCl solution is due to the increased surface coverage as well as increased thickness of adsorbed layer.

The inhibition efficiency from the impedance data was estimated by comparing the values of the R_{ct} in the absence (R°_{ct}) and presence of the inhibitor (R_{ct}) as follows[6]:

$$\%IE = \left(\frac{R^\circ_{ct} - R_{ct}}{R^\circ_{ct}} \right) \times 100 \tag{5}$$

The corrosion inhibition efficiency increases on increasing the concentration of the inhibitor and results obtained are consistent with results obtained from gravimetric as well as potentiodynamic polarization measurements.

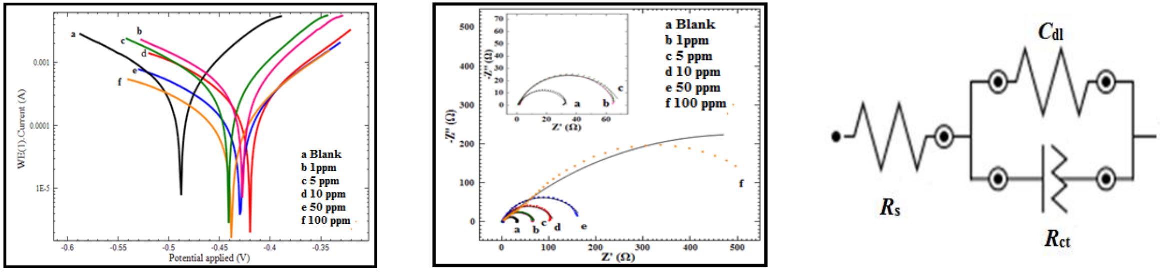

(A) (B) (C)

Figure 1: Typical (A) Tafel, (B) Nyquist plots of MS in 1M HCl in the absence and presence of different concentrations of BPAA, and (C) the suggested equivalent circuit model for the studied system.

Table 1: **PDP and EIS parameters for corrosion of MS in 1M HCl in absence and presence of BPAA at 30±1°C.**

Inhibitor Conc. (ppm)	**PDP**					**EIS**			
	Ecorr (mV)	**icorr ($\mu A/cm^2$)**	**βa (mV/dec)**	**βc (mV/dec)**	**%IE**	**R_s Ohm**	**R_{ct} Ohm**	**C_{dl} μFcm^{-2}**	**%IE**
Blank	-499.97	974.8	135.86	94.006	-	1.4359	33.014		-
1	-420.38	312.87	139.79	98.705	67.91	1.3083	65.055	64.57	49.25
5	-432.26	214.17	170.77	97.969	78.03	1.1117	67.132	56.92	50.82
10	-442.45	174.01	242.79	118.46	82.15	2.5082	105.79	55.15	68.79
50	-438.68	146.38	165.31	90.356	84.99	2.4702	165.76	46.11	80.08
100	-444.49	110.78	310.91	141.56	88.64	10.856	389.21	37.82	91.52

GRAVIMETRIC STUDY

The corrosion inhibiting tendency of the varying concentration of BPAA (1-100 ppm), after 6 h of immersion was studied in 1M HCl at different temperatures (30°-60°C) by using gravimetric technique for MS. The values of the corrosion rate and IE are depicted in Table 2. Both %IE and corrosion rate (CR) increase with rise in temperature as well as increase in the concentration.

Table 2: Corrosion parameters for MS in 1M HCl in absence and presence of different concentrations of BPAA at 30-60°C from gravimetric measurements.

Inhibitor (ppm)	**Corrosion Rate (mgcm^{2}h^{-1})**				**%IE**			
	30°C	40°C	50°C	60°C	30°C	40°C	50°C	60°C
blank	0.824±0.025	2.29±0.098	3.199±0.99	7.851±1.24	-	-	-	-
1	0.597±0.09	1.37±0.015	1.683±0.06	3.717±0.89	27.46	39.91	47.39	52.64
5	0.439±0.03	1.09±0.025	1.319±0.08	2.820±0.98	46.66	52.32	58.78	64.08
10	0.354±0.012	0.707±0.01	0.785±0.057	1.335±0.012	57.09	69.11	75.48	82.99
50	0.247±0.03	0.536±0.011	0.631±0.98	0.968±0.05	69.98	76.56	80.29	87.67
100	0.155±0.041	0.319±0.009	0.284±0.003	0.351±0.01	81.23	86.05	91.13	95.53

ADSORPTION ISOTHERM

The adsorption isotherm experiments were accomplished to have more insights into the mechanism of corrosion inhibition, since it provide information about the interaction among the adsorbed molecules themselves and also their interactions with the electrode surface. The values of *θ* were tested graphically to allow the fitting of a suitable isotherm and the best fit is obtained with Langmuir adsorption isotherm, which is expressed by the following equation[6]:

$$\frac{C_{inh}}{\theta} = \frac{1}{K_{ads}} + C_{inh} \qquad (6)$$

where, C_{inh} is inhibitor concentration and K_{ads} is the adsorption equilibrium constant of adsorption-desorption process. Excellent linear fittings of C_{inh}/θ against C_{inh} plots at 30-60 ^{0}C (Figure 2) with good correlation coefficient (r^2 = 0.999 and nearly unit slope, justifies the applicability of the Langmuir isotherm model at all the studied temperature. The high values of K_{ads} (Table 3) obtained from the intercept of plots indicate that the inhibitor is strongly adsorbed on the MS surface. The standard free energy of adsorption (ΔG^o_{ads}) is related to the adsorption equilibrium constant (K_{ads}) by following equation[16]:

$$\Delta G_{ads} = -RT\ln(1\times10^6\ K_{ads}) \qquad (7)$$

where, 1×10^6 = amount of water molecules expressed in ppm, R is the universal gas constant and T is the absolute temperature. The negative values of ΔG^o_{ads} reveal that the adsorption process takes place spontaneously and the adsorbed layer on the surface of MS is highly stable. It has been widely reported in literature that values of ΔG^o_{ads} of the order of -20 kJ mol^{-1} or less indicate physisorption where the inhibition occurs due to the electrostatic interactions between the charged molecules and the charged metal. ΔG^o_{ads} values of the order of -40 kJ mol^{-1} or more indicate chemisorption, which is due to the charge sharing or a transfer from the inhibitor molecules to the

MS surface to form a co-ordinate type of bond[7]. In our present investigation, the value of the ΔG_{ads} ranges from -30.04 KJ mol^{-1} to -32.09 KJ mol^{-1} suggesting mixed type of adsorption.

Table 3: Values of slope, regression coefficient (R), equilibrium constant (K_{ads}) and free energy of adsorption (ΔG_{ads}) at different temeratures.

Temp	Slope	R^2	K_{ads} ppm mol^{-1}	ΔG_{ads} KJ mol^{-1}
30°C	1.189	0.995	0.1509	-30.04
40°C	1.134	0.997	0.2176	-30.96
50°C	1.077	0.996	0.2501	-31.31
60°C	1.029	0.998	0.3413	-32.09

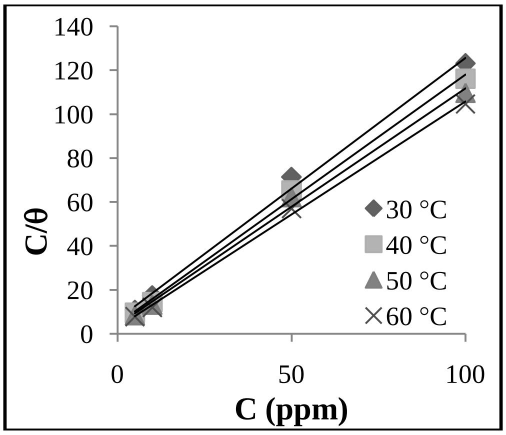

Figure 2: Langmuir adsorption isotherm plots for BPAA adsorbed on MS surface in 1M HCl solution

UV-VIS SPECTROSCOPY

To study the type of interactions of BPAA with the Fe^{2+} in 1M HCl, UV-Vis spectra were recorded for HCl solution comprising 100 ppm of BPAA after and prior to 6 h of MS immersion. The spectrum of pure inhibitor (curve a) showed two main absorption bands around at 250−300 and 340−420 nm, that can be assigned to $\pi \rightarrow \pi^*$ and $n \rightarrow \pi^*$ transitions, respectively (Figure 3). After 6 h of MS immersion (curve b), the bands around 340−420 nm ($n \rightarrow \pi^*$) completely disappeared, and a small downward shift was observed in the band around 250−300 nm. The above observations confirmed the formation of the complex between BPAA and Fe^{2+} ions produced during corrosion reaction of MS in 1M HCl solution.

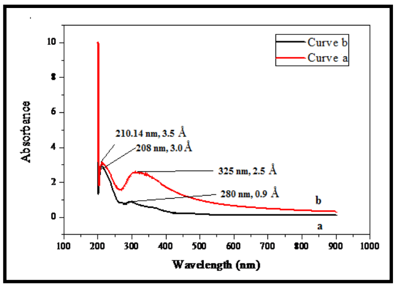

Figure 3: UV–visible spectra of 1 M HCl with 100 ppm BPAA (a) before MS immersion (b) after MS immersion for 6 h at 30°C.

FT-IR SPECTROSCOPY

FT-IR is an effective method for analyzing the films formed on the metal surfaces, which can verify the presence of molecules adsorbed on a surface and provide understanding about the intermolecular environment between films and surfaces. So, in addition to the EDX measurements, FT-IR spectroscopic measurements were conducted to ensure the presence of inhibitor films on the MS surface formed in our experiment. The intermediate infrared spectra ranging from 4000 to 500 cm^{-1} in Figure 4, represents FT-IR spectra of inhibitor and the adsorption film formed on the MS surface after 6 h of immersion time in 1 M HCl solution containing 100 ppm of BPAA, which possesses several functional groups that have high electron density. This implies that the adsorption film between vacant d-orbitals of the metal and BPAA is most likely to take place within these functional groups. The spectrum of pure BPAA (Figure 4 a) shows a characteristic peak at 2925.46 cm^{-1} and 3433.11 cm^{-1} attributed to –NH group and phenyl ring, respectively. A peak at 1638 cm^{-1}, 1407.5 cm^{-1}, 1588.89 cm^{-1} and 1680 cm^{-1} corresponds to –C=O, – CN, Ar-C=C and phenothiazine ring, respectively. The FT-IR spectrum of the film formed on the surface of the MS after 6 h of immersion time in 1 M HCl solution with 100 ppm of inhibitor is shown in Figure 4 b. On comparing the spectrum obtained for the BPAA adsorbed on the MS (Figure 4 b) with the spectrum obtained for the pure BPAA (Figure 4 a) a shift in –phenyl ring and –NH_2 stretching frequencies is observed, which verifies the involvement of these two functional groups in the adsorption of BPAA on the MS surface. The changes in the peaks of –C=O and –CN suggests that these groups are also engaged in the film formation.

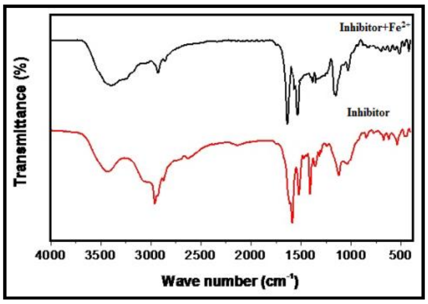

Figure 4: FT-IR spectra of (a) pure BPAA and (b) BPAA adsorbed on the MS surface in 1M HCl.

SEM/EDX

Figure 5 a show the morphology of specimen prior to its immersion in the 1M HCl solution i.e., a freshly polished steel with no noticeable defects except polishing scratches and Figure 5 b show the SEM image of the MS surface after 6 hrs of immersion in the uninhibited 1M HCl which indicates severely corroded surface morphology due to metal dissolution by the corrosive attack of the acid solution while Figure 5 c present images in the presence of 100 ppm of BPAA. In presence of the inhibitor the severity of the acid attack on the MS surface is suppressed due to the formation of a protective covering by the adsorbed inhibitor molecules.

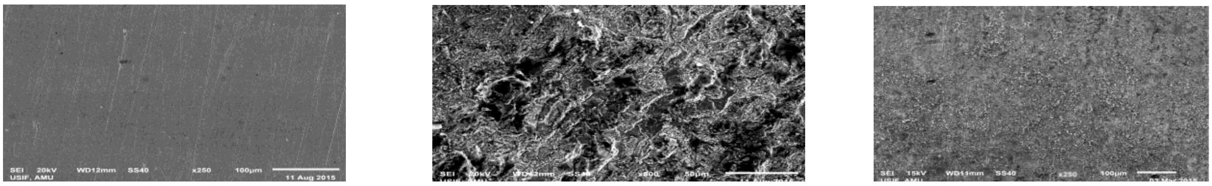

(a) (b) (c)

Figure 5: SEM images of MS surface in 1M HCl after 6 h immersion at 30°C (a) before immersion (polished), (b) after immersion without BPAA, (c) with 100 ppm BPAA

EDX spectra obtained for MS sample in absence and presence of BPAA in 1 M HCl solution are shown in Figure 6 a-c. A prominent peak of iron together with the peaks of other elements constituting the MS are evident on the polished MS surface (Figure 6 a). In the spectrum of MS immersed in an uninhibited acid solution (Figure 6 b) the iron peaks are considerably suppressed (iron content is lowered) and the additional peak of Cl is evident indicating the free corrosion of MS in aggressive acid solution. The spectrum of the MS sample in inhibited acid solution (Figure 6 c) shows the lack of Cl peak and enhancement of carbon signal, which suggest that a protective inhibitor film containing carbon atoms covered the MS surface and prevented the attack from aggressive HCl solution.

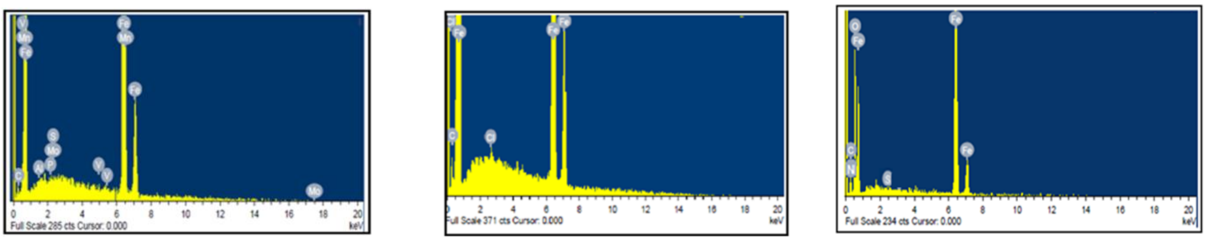

(a) (b) (c)

Figure 6: EDX images of MS surface in 1M HCl after 6 h immersion at 30°C (a) before immersion (polished), (b) after immersion without BPAA, (c) with 100 ppm BPAA

QUANTUM CHEMICAL CALCULATION

Quantum chemical calculations were performed in order to analyse the effect of molecular structure on the performance of the studied inhibitor, as molecular structure of the inhibitor play a vital role in determining its mode of adsorption on the metal surface[7]. The optimized molecular structures, HOMO and LUMO orbitals are given in Figure 7. The computed quantum chemical parameters including the energy of highest occupied molecular orbital (E_{HOMO}), energy of lowest unoccupied molecular orbital (E_{LUMO}), HOMO–LUMO energy gap (ΔE) representing the function of reactivity and total energy (E_t) are represented in Table 4. The energy of the lowest unoccupied molecular orbital (E_{LUMO}) indicates the ability of the molecule to accept electrons; lower the value of E_{LUMO}, the stronger the electron accepting ability of the molecule. The high values of E_{HOMO} are associated with the electron donating ability of the molecule to the empty molecular orbitals. The gap between HOMO–LUMO energy level (energy band gap) of molecules is another important parameter. Smaller the value of ΔE of an inhibitor, higher is the IE of that inhibitor because the excitation energy to remove an electron from the last occupied orbital will be low. The molecules with the high inhibition of corrosion have lower total energy (E_t).

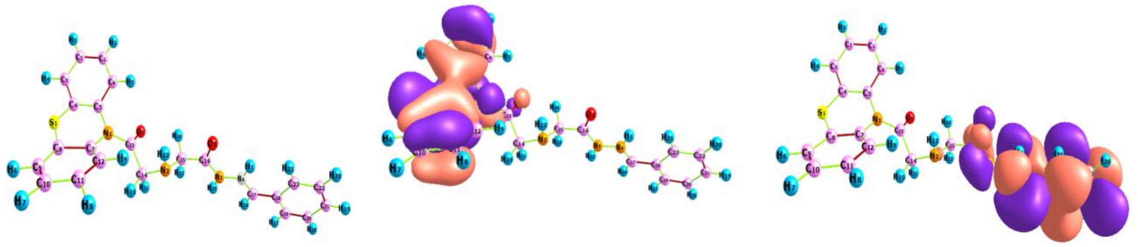

(a) (b) (c)

Figure 7: (a) Optimized molecular structures of GlyC$_3$LS, (b) HOMO and (c) LUMO orbitals

Table 4: Calculated quantum chemical data for BPAA

E_{HOMO} (eV)	**E_{LUMO} (eV)**	**ΔE (eV)**	**E_t (eV)**
-1.62	-5.780	4.16	-45015.48

CONCLUSION

The corrosion inhibition of MS in 1 M HCl solution by BPAA was investigated using electrochemical, gravimetric techniques and theoretical study. Other techniques UV-visible spectroscopic measurements, SEM/EDX were also carried out. The results obtained from the EIS technique indicates that the addition of the BPAA causes an increase in the values of R_{ct} with decrease in the C_{dl}, which suggests that inhibition performance depends on the adsorption of BPAA molecules on the metallic surface and the results of PDP study unveiled that the inhibitor impede both the cathodic and anodic reactions and act as mixed type. On taking account of the results obtained from the gravimetric technique, BPAA act as good corrosion inhibitor with maximum IE of 95.53% at 60 °C with BPAA concentration of 100 ppm. The %IE measured through EIS, potentiodynamic polarization, and gravimetric methods are mutually in good agreement. The inhibition performance is both temperature and concentration dependent. The IE increases with concentration of the inhibitor along with the increase in temperature from 30-60 °C, which is indicative of chemical adsorption. The inhibition occurs through the adsorption of the inhibitor on the MS surface and follows the Langmuir adsorption isotherm at all studied temperature. Thermodynamic parameters unveiled that the adsorption process is comprehensive i.e., involving both physical and chemical adsorption. The results of UV-visible spectroscopic measurements indicates complex formation between inhibitor and Fe^{2+} ions released during corrosion reaction. SEM/EDX images revealed that mild steel surface was effectively protected in inhibited acid solution due to the formation of a protective film by adsorbed inhibitor molecules. Additionally, the analysis of quantum chemical calculations adequately verified the results from the experimental techniques.

ACKNOWLEDGMENT

One of the authors, Saman Zehra acknowledges UGC-MANF, New Delhi for providing financial assistance and USIF-AMU for the facilities provided.

REFERENCES

[1] Tourabi M, Nohair K, Traisnel M, Jama C, Bentiss F, Electrochemical and XPS studies of the corrosion inhibition of carbon steel in hydrochloric acid pickling solutions by 3,5-bis(2-thienylmethyl)-4-amino-1,2.4-triazole, Corros. Sci. 2013;75:123-133.

[2] Abiola OK, James AO, The effects of Aloe vera extract on corrosion and kinetics of corrosion process of zinc in HCl solution, Corros. Sci. 2010;52:661-664.

[3] Yildiz R, An electrochemical and theoretical evaluation of 4, 6-diamino-2-pyrimidinethiol as a corrosion inhibitor for mild steel in HCl solution, Corros. Sci. 2015;90:544-553.

[4] Oguzie EE, Li Y, Wang SG, Wang F, Understanding corrosion inhibition mechanism-experimental and theoretical approach, RSC Adv. 2011;1:866-873.

[5] Hegazy MA, Badawi AM, Rehim SSAE, Kamel WM, Corrosion inhibition of carbon steel using novel N-(2-(2-mercapto acetoxy)ethyl)-N, N-dimethyl) dodecan-1-aminium bromide during acid pickling, Corros. Sci. 2013;69:110-122.

[6] Mobin M, Zehra S, Parveen M, L-Cysteine as corrosion inhibitor for mild steel in 1MHCl and synergistic effect of anionic, cationic and non-ionic surfactants, J. Mol. Liq. 2016;216:598-607.

[7] Mobin M, Zehra S, Aslam R, L-Phenylalanine methyl ester hydrochloride as a green corrosion inhibitor for mild steel in hydrochloric acid solution and the effect of surfactant additive, RSC adv. 2016;6:5890–5902.

[8] Ismail KM, Evaluation of cysteine as environmentally friendly corrosion inhibitor for copper in neutral and acidic chloride solutions, Electrochim. Acta. 2007;52:7811–7819.

[9] Oguzie EE, Li Y, Wang FH, Corrosion inhibition and adsorption behavior of methionine on mild steel in sulfuric acid and synergistic effect of iodide ion, J. Colloid Interface Sci. 2007;310:90–98.

[10] Mobin M, Parveen M, Rafiquee MZA, Inhibition of mild steel corrosion using l-histidine and synergistic surfactants additives, J. Mater. Eng. Perform. 2013;22:548-556.

[11] Bostan R, Varvara S, Popa M, Muresan LM, Evaluation of phenothiazine as environmentally friendly corrosion inhibitor for bronze in synthetic acid rain, Studia UBB chemia. 2013;3:53-62.

[12] Yadava M, Kumara S, Gope L, Experimental and theoretical study on amino acid derivatives as eco-friendly corrosion inhibitor on mild steel in hydrochloric acid solution, journal of adhesion science and technology, J. Adhes. Sci. Technol. 2014;28:1072–1089.

[13] Natha SP, Yadav MK, Laxmi T, Synthesis and anticonvulsant activity (chemo shock) of phenothiazine amino acid derivatives, Chem Sci Trans. 2013;2:123-128.

[14] Sorkhabi HA, Majidi MR, Seyyedi K, Investigation of inhibition effect of some amino acids against steel corrosion in HCl solution, Appl. Surf. Sci. 2004;225:176–185.

[15] Barouni K, Bazzi L, Salghi R, Mihit M, Hammouti B, Albourine A, Issami SE, Some amino acids as corrosion inhibitors for copper in nitric acid solution, Mater. Lett. 2008;62:3325–3327.

[16] Solomon MM, Umoren SA, In-situ preparation, characterization and anticorrosion property of polypropylene glycol/silver nanoparticles composite for mild steel corrosion in acid solution, J. Colloid Interface Sci. 2016;462:29–41.